2012 IEEE International Conference on Robotics and Automation
RiverCentre, Saint Paul, Minnesota, USA
May 14-18, 2012

Powered Wheelchair Navigation Assistance through Kinematically Correct Environmental Haptic Feedback

E.B. Vander Poorten, E. Demeester, E. Reekmans, J. Philips, A. Hüntemann and J. De Schutter

***Abstract*— This article introduces a set of novel haptic guidance algorithms intended to provide intuitive and reliable assistance for electric wheelchair navigation through narrow or crowded spaces. The proposed schemes take hereto the non-holonomic nature and a detailed geometry of the wheelchair into consideration. The methods encode the environment as a set of collision-free circular paths and, making use of a model-free impedance controller, 'haptically' guide the user along collision-free paths or away from obstructed paths or paths that simply do not coincide with the motion intended by the user. The haptic feedback plays a central role as it establishes a fast bilateral communication channel between user and wheelchair controller and allows a direct negotiation about wheelchair motion. If found unsatisfactory, suggested trajectories can always be overruled by the user. Relying on inputs from user modeling and intention recognition schemes, the system can reduce forces needed to move along intended directions, thereby avoiding unnecessary fatigue of the user. A commercial powered wheelchair was upgraded and feasability tests were conducted to validate the proposed methods. The potential of the proposed approaches was hereby demonstrated.**

I. Introduction

Powered wheelchairs are built to assist people with physical and/or cognitive limitations in their daily life. They help to solve the loss in independence experienced by individuals that suffer from restricted mobility. By doing so they have a direct impact on the quality of life of their users. Unfortunately, not everyone is able to benefit from this technology. The relatively large dimensions of wheelchairs compared to the size of everyday environments makes maneuvering difficult. Seemingly simple maneuvers such as doorpassing or taking an elevator require considerable motor and cognitive skills. The limited response speed and large inertia of these systems can lead to dangerous situations, possibly inflicting serious harm upon the driver or bystanders.

For this reason, so-called 'smart' wheelchairs are being developed since the early eighties. These systems try to simplify navigation tasks and assist in transporting the user safely to a desired location [1]. Some of the more advanced systems such as TAO, the NavChair, Rolland or the SmartChair foresee multiple assistance modes that are switched depending on the context. Such systems partially take over the control from the user and adjust the user's inputs by providing assistance for wall-following, collision avoidance or door-passage tasks. Since the user only perceives the decisions by the navigation system *after* wheelchair displacement, such approaches might unexpectedly cause frustration and actually complicate maneuvering tasks. For instance this is the case when the provided assistance does not correspond to the needed or the expected assistance. The latter is often referred to as *mode confusion* in the literature [2], [3]. Shared control approaches that follow this pattern (Fig.1) exhibit a certain asymmetry in the decision making process and will be referred to as *unilateral* shared control approaches hereafter. With good knowledge of the wheelchair behaviour the user might be able to anticipate the wheelchair's response. Yet, in complex or adaptive assistive schemes this is an error-prone and possibly dangerous process.

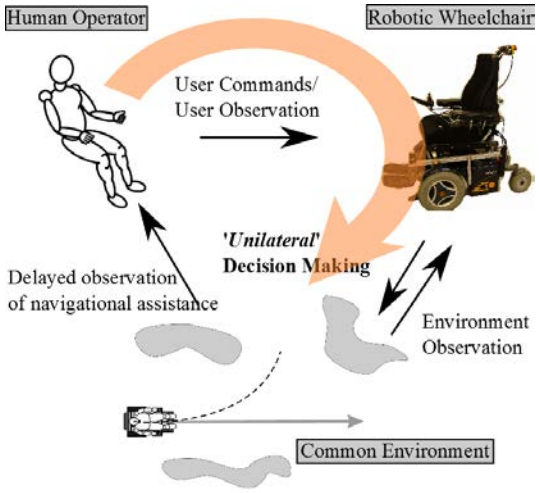

Fig. 1: Traditional shared control schemes display asymmetry in the decision making process. Users only understand decisions after actual displacement took place.

Parallel to advances in mobile navigation teleoperation tasks [4], researchers started recently to experiment with haptic feedback for wheelchair navigation [5]–[13]. By setting up a fast, *bilateral* communication channel between the user and the wheelchair controller, control can be shared more profoundly (Fig.2). The user can directly negotiate with the controller over this haptic channel and is given the final word, as he/she can *overrule* unwanted wheelchair actions. Next to challenges in designing robust haptic display hardware for this application, a major challenge remains in the design of intuitive bilateral shared control methods that fully exploit the opportunities of the haptic channel and

E.B. Vander Poorten, E. Demeester, J. Philips, A. Hüntemann and J. De Schutter are with the Dept. of Mechanical Engineering, KU Leuven, 3001 Heverlee, Belgium Emmanuel.VanderPoorten@mech.kuleuven.be

E. Reekmans is employed by Intermodalics, a KU Leuven spin-off developing automation solutions, 2040 Berendrecht, Belgium eli.reekmans@intermodalics.eu

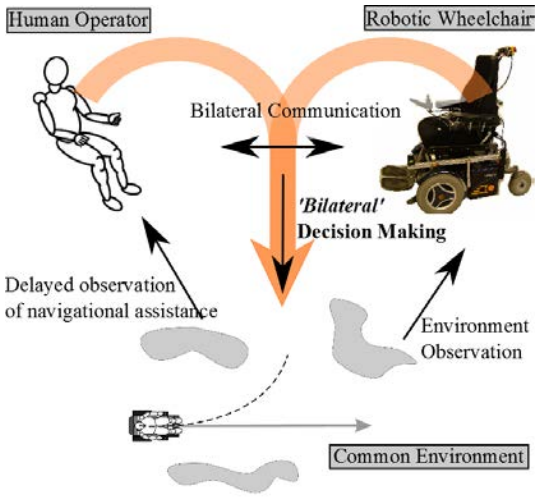

Fig. 2: Bilateral shared control schemes feature a deeper level of control sharing, allowing the user to negotiate directly with the wheelchair over a haptic communication channel.

that do not cause additional fatigue of its user. This article presents a novel approach for haptic navigation assistance that uses environmental information in the form of collision-free circular paths. The approach is designed so that in a later stadium estimated intentions and wheelchair dynamics can be easily embedded in this framework. The paper is organised as follows. Section II gives a brief overview of prior art in haptic guidance for navigation assistance and explains the fundamentals of the novel approach. Section III describes the proposed control algorithm in more detail. From this general scheme a number of assistance strategies are derived in IV. In section V the practical setup and a novel haptic display system are shortly described. Some initial experiments are reported in section VI to demonstrate the potential benefit of the proposed approach. Finally, conclusions and directions for future research are put forward in section VII.

II. Improved Navigational Assistance through Haptic Guidance

A. State of the art of haptic guidance for wheelchair navigation

The rotational and translational velocity of normal electric wheelchairs (v,ω) are roughly proportional to the deviation (x,y) of a joystick from its neutral position (Fig.3). The idea of haptic guidance is to encode various sources of information and to combine this into a single 2-dimensional force signal (F_x,F_y) applied through a force feedback joystick to the user. This signal should guide joystick motion towards 'likely' joystick positions (and corresponding wheelchair motion) and adversely prevent motions towards 'unlikely' directions. Prior art can be subdivided in the type of information that is encoded and the manner how this information is encoded. So far, most attention went to devise intuitive schemes to feed 'environmental information' back to the user. Hong *et al.* propose a 'virtual elasticity zone' around the vehicle [5]. Obstacles in this zone generate opposing forces proportional to the intrusion depth into the

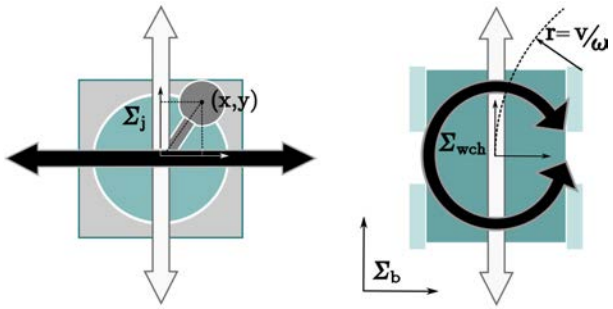

Fig. 3: One to one mapping of joystick position (left) to wheelchair velocity (right). Each position (x,y) expressed in joystick coordinate frame Σ_j corresponds to a linear and rotational velocity (v,ω) w.r.t. local wheelchair coordinate frame Σ_{wch}, resulting in an instantaneous circular path with radius $r=v/\omega$ in base coordinate frame Σ_b.

elasticity zone. Protho *et al.* additionally scale forces with increasing wheelchair velocity [7]. Fattouh calculates forces as a weighted sum of directional forces inversely proportional to the distance to obstacles [11]. Kitagawa *et al.* control the joystick impedance as a function of (holonomous) wheelchair velocity and distance to obstacles [8]. In addition to 'environmental feedback' forces, Lee embeds the wheelchair size into the collision avoidance strategy. Additional collision-preventing forces are parameterized in function of maximal frontal and backward collision-free distance, and maximal clockwise and counterclockwise collision-free rotation [12], [14]. The Generalised Potential Field (GPF) scheme by Krogh *et al.* considers the limits on vehicle deceleration as adapted for haptic feedback by Boschloo *et al.* [10]. Factors such as vehicle dimensions (circumscribed circle), safety zone and user reaction time were accounted for.

Since purely reactive schemes tend to fatigue the user too much, specially in cluttered spaces, Hong introduced Gaussian filters to reduce the effect of obstacles that do not lie in the direction of wheelchair motion [5]. Such filters are also used by Luo *et al.*, who further try to reduce user effort by programming attractive forces in directions where free space is perceived [6]. Recently, Bourhis and Sahnoun employed the vector field histogram and the minimal vector field histogram [15] methods to determine a free direction within surrounding obstacles. Then, they provide haptic guidance to move towards these free directions [13].

B. Concept of novel algorithm

The novel algorithm proposed in this paper is based upon the following observations:

1) prior art ignores the non-holonomic nature of most powered wheelchairs, although this has important implications on the effectiveness of haptic guidance schemes.
2) prior art does not (sufficiently) take wheelchair geometry into account where in daily life a few centimeters can make a difference between passage or collision.
3) prior assistance schemes are mainly geometric, hardly considering user characteristics nor intentions, although

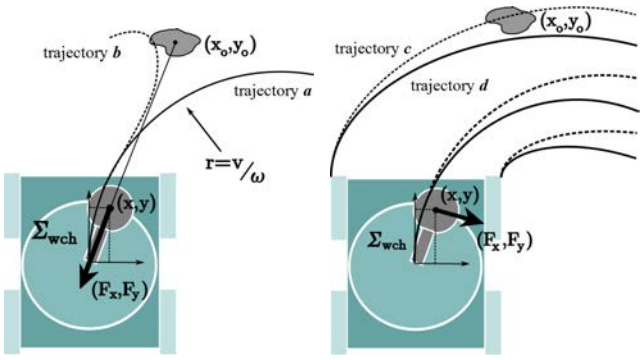

(a) Effect of non-holonomicity on wheelchair motion.

(b) Effect of wheelchair geometry on passage.

Fig. 4: Need to incorporate accurate kinematic wheelchair model into haptic guidance algorithms.

such knowledge could help shaping schemes that trade-off better between guiding and tiring a specific user.

Typically, in prior art, environmental obstacles located e.g. at (x_o, y_o) in the wheelchair's local coordinate frame Σ_{wch} generate repulsive forces (F_x, F_y) in the opposite direction (of the same local frame Σ_{wch}[1]). Such forces can be misleading and even inappropriate as joystick displacement results in new linear and rotational wheelchair velocity (v, ω) rather than in translational velocity (v_x, v_y).

Fig.4a sketches how reactive schemes that do not account for the nonholonomic nature of the wheelchair would 'needlessly' slow down the wheelchair and bend an otherwise collision-free path trajectory a, that corresponds to a constant joystick position (x, y), towards a second path trajectory b, causing additional fatigue of its user. Fig.4b shows how wheelchair geometry is to be taken into account to avoid collision with an object at (x_o, y_o) and how haptic guidance can be used to bend trajectory c into a collision-free trajectory d. Prior work [16], [17] reveals how user modelling and intention estimation for wheelchair navigation can assist in wheelchair navigation. Haptic guidance strategies that incoporate this information can provide more effective guidance to the user potentially reducing navigation effort and fatigue.

The next section presents a novel approach for haptic guidance that encodes environmental information and arbitrary wheelchair geometry in the form of collision-free circular paths. Based on this encoding a time-varying impedance controller is designed to guide the user instantaneously along a collision-free trajectory. This scheme can be easily expanded to incorporate knowledge from user modelling by simply lowering the impedance in directions that correspond to estimated user intentions.

III. Novel scheme for haptic navigation guidance

A. Environment encoding as a set of collision-free paths

a) Generation of circular paths: In case the dynamic effects of the wheelchair are negligible, general wheelchair motion can be approximated as a sequence of instantaneous motions on circular paths $\mathscr{C}_m$ w.r.t. a base coordinate frame Σ_b. The radius r of such path $\mathscr{C}_m$ is, for joystick position (x, y) and corresponding velocity commands

$$\begin{aligned} v &= k_v y, \\ \omega &= -k_\omega x \end{aligned} \tag{1}$$

with appropriate velocity gains k_v and k_ω, given by:

$$r = |v|/|\omega|. \tag{2}$$

As long as the joystick position does not change, the wheelchair will move along the same circle $\mathscr{C}_m$. In fact, *all* joystick positions on a line through the origin of Σ_j and position (x, y), thus forming an angle ϕ_m with the X-axis of Σ_j, will command the wheelchair to move along $\mathscr{C}_m$, albeit with different speeds. This can be easily verified by noting that for arbitrary points (x_1, y_1) and (x_2, y_2) on such line

$$\tan(\phi_m) = \mathrm{C^{te}} \;\Rightarrow\; \frac{y_1}{x_1} = \frac{y_2}{x_2} \tag{3}$$

and that from (1) and (2) follows that

$$r_1 = \frac{|v_1|}{|\omega_1|} = \frac{|k_v y_1|}{|k_\omega x_1|} = \frac{|k_v y_2|}{|k_\omega x_2|} = \frac{|v_2|}{|\omega_2|} = r_2. \tag{4}$$

The path associated with (x_1, y_1) and (x_2, y_2) is thus the same. By extension all two-dimensional joystick positions can be encoded as a one-dimensional set of circular paths:

$$\begin{aligned} &r_m = \left| \frac{k_v}{k_\omega} \tan(m\Delta\phi) \right|, \quad \text{for } m = 0, \ldots, N-1 \text{ and } N \in \mathbb{Z}_0^+ \\ &\text{and} \quad \Delta\phi = \frac{2\pi}{N-1} \quad \text{where } N \to \infty. \end{aligned} \tag{5}$$

Each circular path segment is represented as a (v, ω, dt) tuple where the path's length equals $v \cdot dt$ and the orientation change $\omega \cdot dt$. Note that $m\Delta\phi = \{0, \pi\}$ corresponds to pure rotational motion, whereas $m\Delta\phi = \{\pi/2, 3\pi/2\}$ corresponds to pure translational motion. For computational reasons it is necessary to discretize the set of possible circular paths by using a finite value for N. In this work N is set to 144. It can be appreciated that, after selecting a discretization method for the arclength and a number of steps M to proceed along the arc, the geometry and coordinates of all the $M \times N$ points over the N circular paths is invariable in Σ_j. These points can thus be precomputed and stored in a look-up table to speed up further calculations.

b) Determining collision-free lengths of circular paths: Next, the distance over each circular path until first collision with the environment is computed.

1) A local map of the environment is built and refined at a fixed update rate. Ranging data from laser (or other) sensors can be used to build an online map of the environment expressed relative to the wheelchair local coordinate system Σ_{wch}. Prior information of the environment, transformed from Σ_b to Σ_{wch}, can be used to improve the accuracy of the local map (Fig.5a).
2) In a following step, intersections are checked between the local environment and the wheelchair moving over all circular paths. The wheelchair geometry is hereto

[1]For simplicity and without loss of generality $\Sigma_j = \Sigma_{wch}$ is assumed here.

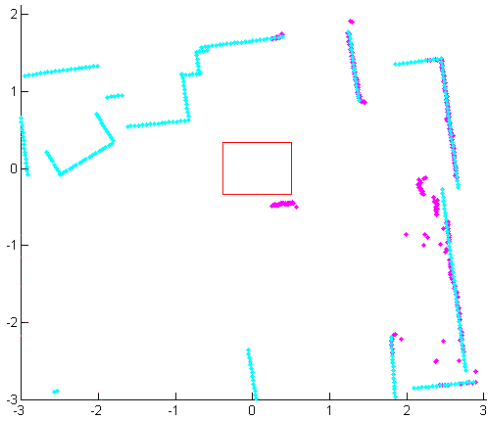

(a) 2D map of the environment, using real-time sensor information (dark purple marks) and prior knowledge (light cyan marks). The central rectangle represents the wheelchair.

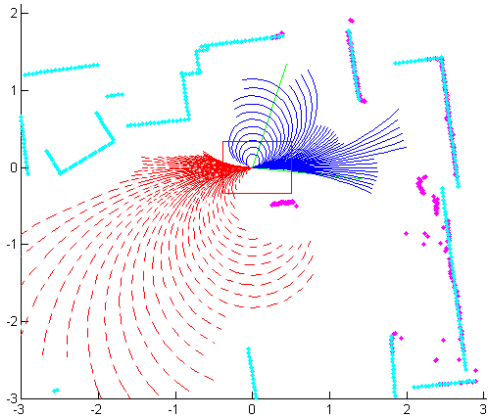

(b) Circular collision-free paths, calculated from the map and wheelchair geometry. Blue arcs represent forward paths, red dashed lines are backward paths.

Fig. 5: Collision-free paths of wheelchair in its surroundings

shifted at a predefined speed (v,ω) over each circular path and the earliest time of intersection dt is recorded. This time, representative for the collision-free length, is stored in an $N \times 1$ vector.

Fig.5b shows the collision-free paths that are calculated for the wheelchair based on environmental data from Fig.5a. The haptic guidance is then programmed so that the wheelchair follows one of these paths, preferably the one closest to the wheelchair driver's intention. Based on new sensor readings, maps and collisions are recomputed, forces recalculated and so on. The next section explains in greater detail the actual implementation of the haptic guidance algorithms.

B. Haptic control algorithms based on collision-free lengths

c) Adaptive model-free impedance control: A model-free impedance controller with inner force feedback loop is chosen to regulate the haptic interaction [18], [19]. Fig.6 depicts a block scheme of the controller. The aim is to replicate the feeling of a desired impedance $\mathbf{Z}_{perceived} = \mathbf{Z}_d$ at the end-effector of the joystick, with $\mathbf{Z}_{perceived} = \mathbf{Y}^{-1}_{perceived}$ indicated on Fig.6. The inner force feedback loop, encompassing

- the joystick itself, represented by admittance $\mathbf{Y}_{joy}$,

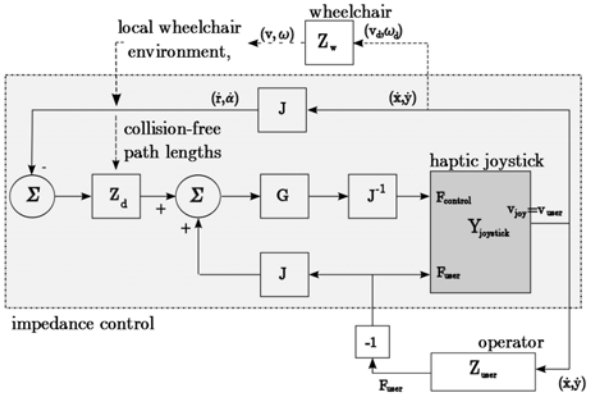

Fig. 6: Impedance controller providing haptic guidance along collision-free paths.

- the human operator holding the joystick, $\mathbf{Z}_{user}$, whose behaviour is captured through measurement of forces $\mathbf{F}_{user}$ and velocity estimates $\mathbf{v}_{user}$, and
- force feedback gains $\mathbf{G}$,

allows to compensate the inherent dynamics (inertia, damping, friction) of the joystick so that $\mathbf{Z}_{perceived}$ approaches $\mathbf{Z}_d$. It further allows one to set $\mathbf{Z}_d$ very low. With a large share of wheelchair users suffering from fatigue, unable to supply large forces, this property is especially important.

d) Transformation to polar coordinate system: The haptic guidance is now programmed by designing impedances $\mathbf{Z}_d$. A good design strategy is crucial to obtain intuitive and safe navigation assistance. Recalling the mapping from joystick positions to circular paths (section III-A), it is more natural to express $\mathbf{Z}_d$ in a polar coordinate system, rather than in the original Cartesian frame Σ_j. Hereto

$$\begin{aligned} \rho &= \sqrt{x^2+y^2}, \\ \phi &= \text{atan}(y,x), \end{aligned} \tag{6}$$

is applied. The variation $\partial \mathbf{Z}_d / \partial \rho$ explains then the change in impedance felt when changing travel speed along a circular path. The variation $\partial \mathbf{Z}_d / \partial \phi$ corresponds to the change in impedance that is felt when the user wants to change lane towards a different circular path. Note that since forces and velocity measurements take place in Cartesian space, jacobian matrices J, containing derivatives of (6) appear in the block scheme of Fig.6.

e) Mapping collision-free lengths to impedances: Supplied with a vector of path lengths dt from subsection III-A, a natural encoding is then to attribute higher resistance to paths with short collision-free paths and vice versa. Since dt is a function of the angle ϕ, so is $\mathbf{Z}_d$. In practice, the variable resistance is thus fed back under the form of a variable joystick stiffness k_{dt}.

Table I indicates how k_{dt} is calculated as a function of dt. A path length above dt_{max} is considered infinite and receives minimal stiffness k_{min}. A path length below dt_{min} corresponds to a maximal stiffness k_{max}. In between, a lineair relationship between dt en k_{dt} is imposed. Knowledge about the user's intention (probabilities over the paths) could in

the future be used to modify the stiffness associated with a certain path. When a user finds himself for example in front of a closed door, the path lengths will be short and consequentially a high stiffness will be displayed. However, in case the user persists in moving in that direction the system, becoming more sure about the user's intention, can then reduce the displayed stiffness. Next to the variable stiffness a small constant damping c and inertia equal to zero form the desired virtual dynamics $\mathbf{Z}_d$. The Laplace form of the virtual dynamics is therefore given by

$$\mathbf{Z}_d(s) = \frac{\mathbf{k}(\phi)}{s} + \mathbf{b}. \tag{7}$$

To accommodate for the effect of sensor noise and differences in loop rates a number of additional processing steps is needed before obtaining the actual forces that will be commanded towards the haptic joystick's motors. These steps are explained next.

f) Smoothening environmental data: To avoid that big jumps in path lengths caused by sensor noise, produce sudden jumps in impedances/and output forces, the path length vector is filtered with a Gaussian convolution mask. A for-loop is programmed, in which an original n-dimensional vector $\mathbf{q} \in \Re^{n\times 1}$ gets shifted a limited number of steps to the front (resulting in $\mathbf{q}^+$) and to the back (resulting in $\mathbf{q}^-$) every run through. The convoluted vector $\mathbf{q}_c$ is then obtained as indicated in Table II. Convoluted vectors for $\mathbf{dt}_c$ were calculated in this manner with $\sigma = 5$ and $j = 14$ being experimentally determined.

g) Upsampling towards haptic update rates: Since humans can perceive force variations up to high frequencies (Tan *et al.* report up to 1000Hz [20]), haptic control loops rates are typically run at 1kHz or higher, which is two orders of magnitude faster than the environmental perception loop that runs here at 10Hz. To accommodate for the difference in loop rate, the slower signals are upsampled by linearly extrapolating the last two measurement values until a 1kHz rate. This approach introduces thus a delay of 100ms which is acceptable for such relatively slowly varying property.

TABLE I: Algorithm 1

Calculating stiffness k_{dt} from path length dt

Input: dt
Output: k_{dt}

if $(dt \geq dt_{max})$
  $k_{dt} = k_{min}$;
else if $(dt \leq dt_{min})$
  $k_{dt} = k_{max}$;
else
  $k_{dt} = k_{min} + \frac{k_{min}-k_{max}}{dt_{max}-dt_{min}} \cdot (dt - dt_{max})$;

TABLE II: Algorithm 2

Algorihtm 2: Gaussian convolution mask, applied to vector $\mathbf{q}$

Input: $\mathbf{q}, j, \sigma$
Output: $\mathbf{q}_c$

$\mathbf{q}_c = \frac{1}{\sigma\sqrt{2\pi}}\mathbf{q}$
for $m = 1$ to j
  $\mathbf{q}^+ \leftarrow [\mathbf{q}(n-m+1\cdots n); \mathbf{q}(1\cdots n-m)]$;
  $\mathbf{q}^- \leftarrow [\mathbf{q}(m+1\cdots n); \mathbf{q}(0\cdots m)]$;
  $g \leftarrow \frac{1}{\sigma\sqrt{2\pi}} exp\left(-\frac{m^2}{2\sigma^2}\right)$;
  $\mathbf{q}_c \leftarrow \mathbf{q}_c + g\cdot(\mathbf{q}^+ + \mathbf{q}^-)$;
end for

$\mathbf{q}_c \leftarrow \frac{max(\mathbf{q})}{max(\mathbf{q}_c)}\mathbf{q}_c$;

IV. Different user modes with haptic guidance

Based on the scheme developed in section III, two different operation modes are derived next. The proposed schemes can be seen as haptic equivalents of the more traditional collision avoidance and obstacle avoidance schemes.

A. Collision avoidance

In collision avoidance mode, the navigation assistance limits itself to slowing down the wheelchair and coming to a full stop in front of an obstruction. This assistance mode does not try to change the wheelchair's path, so only the radial component of the impedance $\mathbf{Z}_d$ is used. The joystick behaves then as a spring-damper connected to the origin of the joystick coordinate frame Σ_j. The stiffness $k(\phi)$ is function of the joystick angle ϕ, but independent of ρ. The exerted force varies linearly with magnitude ρ as in

$$F_\rho = \begin{cases} -F_{\rho,0} - k(\phi)\cdot\rho - b_\rho\cdot\dot{\rho} & \text{for} \quad \rho \geq \rho_{nz} \\ -b_\rho\cdot\dot{\rho} & \text{for} \quad \rho < \rho_{nz} \end{cases} \tag{8}$$

and is always directed towards the center of the joystick. b_ρ is the radial component of damping $\mathbf{b}$ in (7). For stability reasons a neutral zone with radius ρ_{nz} is programmed around the midpoint in (8). Offset $F_{\rho,0}$ is such that $F_\rho|_{(\rho=\rho_{nz})}$ is zero, when $\dot{\rho} = 0$. Fig.7a illustrates an exemplary force field when an obstacle is detected on the righthand side of the wheelchair and k is calculated as k_{dt} of Table I.

B. Obstacle avoidance

Obstacle avoidance schemes bend the wheelchair motion towards an alternative path, helping it to pass an obstacle rather than simply slowing it down. This behaviour is realised by employing both radial and tangential components of $\mathbf{Z}_d$. The former corresponds to (8), the latter can be approximately calculated with central finite differences from the surrounding stiffness values as in

$$F_{\phi_m} = \begin{cases} -F_{\phi_m,0} - \frac{k_{m+1}-k_{m-1}}{\phi_{m+1}-\phi_{m-1}}\cdot\rho - b_\phi\cdot\dot{\phi} & \text{for} \quad \rho \geq \rho_{nz} \\ -b_\phi\cdot\dot{\phi} & \text{for} \quad \rho < \rho_{nz} \end{cases} \tag{9}$$

for b_ϕ the tangential component of damping b in (7) and a joystick angle $\phi_m \in [(m-1/2)\Delta\phi, (m+1/2)\Delta\phi)$ for $m = 0,\ldots,N-1$, with $\Delta\phi$ defined in (5). Note that to avoid overly complex notations, the special cases $m = 0, N$ are ignored in (9). The offset F_{ϕ,m_0} is a constant such that $F_{\phi_m}|_{(\rho=\rho_{nz})}$ is zero, when $\dot{\phi} = 0$. Fig. 7b illustrates the gradients of the force field of Fig.7a.

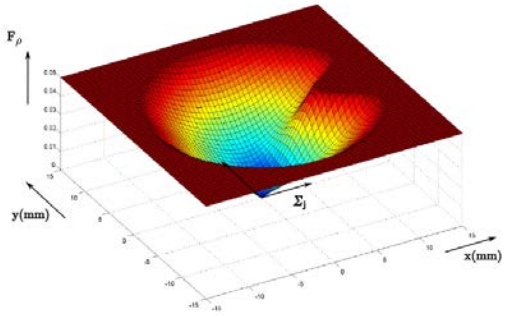

(a) Exemplary force field F_ρ generated in collision avoidance mode when an obstacle is detected on the righthand side of the wheelchair. The vertical axis shows the force amplitude, with upperbound F_{max} implemented for safety reasons. The force is always directed towards the midpoint $(0,0)$ of Σ_j.

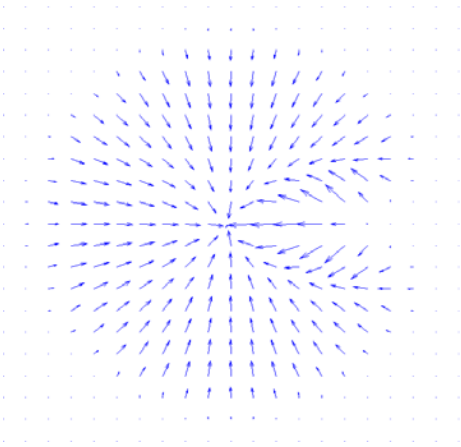

(b) The gradients of the force field F_ρ indicating the direction and the magnitude of forces generated in obstacle avoidance mode when an obstacle is located at righthand side of the wheelchair.

Fig. 7: Force patterns generated under collision and obstacle avoidance modes

V. Practical Setup

To validate the proposed algorithms a test setup was built around the commercial powered wheelchair depicted in Fig.8. A metal frame was added to the wheelchair to mount additional hardware. Two Hokuyo URG-04LX laser sensors with each a field of view of 270° were placed at diagonal corners of this frame. In this way a full 360° 2-dimensional scan of the surroundings of the wheelchair is captured at once. The coverage of each Hokuyo is marked in colour on Fig.8. A host computer mounted at the back of the seating reads out the laser scanners and builds up 2D maps of the environment. The host computer (Windows OS) communicates over UDP with a NI CompactRIO 9074 central processing unit (cRIO). Labview RT, a real-time OS based upon VxWorks, is installed on this embedded PC. The haptic control loop runs here at a rate of 1kHz.

A recent in-house designed 2-d.o.f. haptic joystick is mounted in line with the armrest of the wheelchair. This is a compact and powerfull joystick showing high continuous output force at the handle (up to 40N, thanks to 2 Maxon RE30 motors, a cable-based reduction mechanism

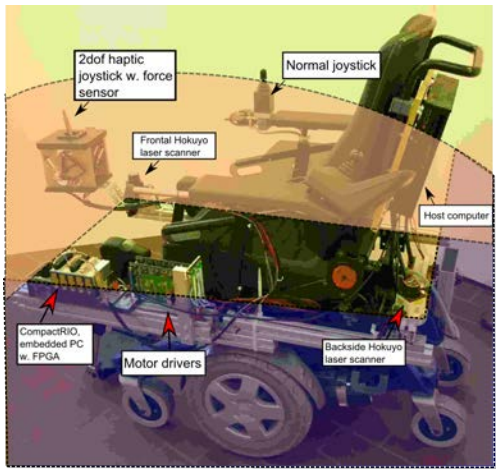

Fig. 8: Commercial powered wheelchair interfaced and upgraded for providing haptic navigation assistance.

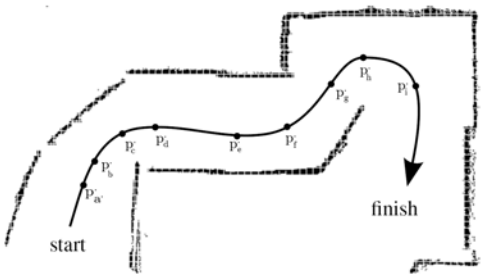

Fig. 9: Users follow a trail enclosed by cardboard boxes

with 1 : 10 reduction ratio and Maxon ADS_E 50/5 PWM current-controlled motor drives). Also, high resolution position measurement (Scancon 2RMHF5000, 20.000 p.p.r. after quadrature encoding) and interaction forces measurements (HBM, 1-LY11-1.5/120 strain gauges glued on the joystick handle) are available. To test the algorithms a corridor was built by placing a number of cardboard boxes. Fig.9 shows the map that was constructed of this artificial environment.

VI. Experiments

Some initial experiments were conducted to validate the proposed haptic guidance algorithms by driving with the wheelchair along the trajectory of Fig.9. In these experiments a user was asked to follow the trail illustrated in Fig.9. The experiment was done once with a constant stiffness profile, making the joystick feel like a traditional joystick; once using the collision-avoidance user mode and once using the obstacle-avoidance user mode. A local map of the environment was constructed and collision-free paths calculated. Fig.(10a-10h) depict the calculated collision-free paths and associated force fields in selected points along the path. It can be observed that the user is effectively guided haptically alongside the path. Note that at places where the corridor is sufficiently broad, no resistance is present against performing a U-turn. These preliminary tests show the potential of the proposed schemes to help establish a good balance between user guidance and leaving the user the freedom to steer the chair in the desired direction.

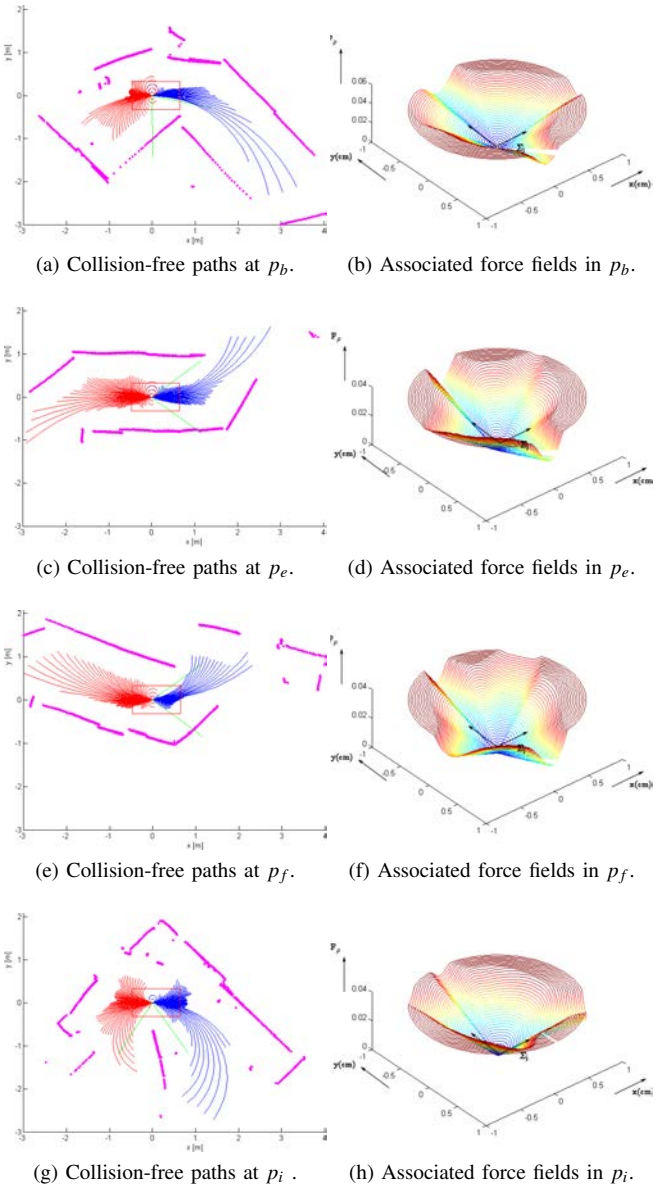

(a) Collision-free paths at p_b. (b) Associated force fields in p_b.

(c) Collision-free paths at p_e. (d) Associated force fields in p_e.

(e) Collision-free paths at p_f. (f) Associated force fields in p_f.

(g) Collision-free paths at p_i . (h) Associated force fields in p_i.

Fig. 10: Navigation assistance at selected points along the path of Fig.9.

VII. Conclusions and Future Works

This paper presented a new set of haptic guidance algorithms for wheelchair navigation assistance that haptically feed back environmental information, encoded under the form of circular collision-free paths, to its user. The novel algorithms take into account the non-holonomic nature of the wheelchair as well as precise geometric knowledge of the wheelchair's dimensions (in 2D). This property allows improved navigational assistance through narrow passages compared to schemes that do not consider this information. Extensions that incorporate wheelchair dynamic behaviour and user intention can improve navigation accuracy further, potentially reducing user fatigue. Further research will be directed towards finetuning the control scheme's parameters and integrating intention recognition algorithms.

VIII. Acknowledgments

This research was conducted in the framework of the RADHAR project, funded by the European Commission's 7th Framework Programme FP7/2007-2013 Under grant agreement No.248873 and under support of a Marie Curie Reintegration Grant, PIRG03-2008-231045.

References

[1] R. C. Simpson, "Smart wheelchairs: A literature review." *J Rehabil Res Dev*, vol. 42, no. 4, pp. 423–436, 2005.

[2] T. Sheridan, *Telerobotics, Automation and Human Supervisory Control*. Cambridge, Massachusetts, and London, England: The MIT Press, 1992.

[3] A. Lankenau, "Avoiding mode confusion in service robots - the bremen autonomous wheelchair as an example," in *Proc. of the 7th Int. Conf. on Rehabilitation Robotics (ICORR'2001)*, Evry, France, apr 2001, pp. 162–167.

[4] T. Fong, F. Conti, S. Grange, and C. Baur, "Novel Interfaces for Remote Driving: Gesture, Haptic and PDA," in *SPIE Telemanipulator and Telepresence Technologies VII*, 2000.

[5] J.-P. Hong, O.-S. Kwon, E.-H. Lee, B.-S. Kim, and S.-H. Hong, "Shared-control and force-reflection joystick algorithm for the door passing of mobile robot or powered wheelchair," in *Proc. IEEE Region 10 Conference TENCON 99*, vol. 2, 1999, pp. 1577–1580 vol.2.

[6] R. Luo, C. Hu, T. Chen, and M. Lin, "Force reflective feedback control for intelligent wheelchairs," in *Proc. IEEE/RSJ Int. Conf. Intel. Rob. and Syst.*, 1999, pp. 918–923.

[7] J. Protho, E. LoPresti, and D. Brienza, "An evaluation of an obstacle avoidance force feedback joystick," in *Conf. of Rehabilitation Engineering and Assistive Technology Soc. of North America*, 2000.

[8] H. Kitagawa, T. Kobayashi, T. Beppu, and K. Terashima, "Semi-autonomous obstacle avoidance of omnidirectional wheelchair by joystick impedance control," vol. 4, 2001, pp. 2148–2153 vol.4.

[9] S. Lee, G. Sukhatme, G. Kim, and C.-M. Park, "Haptic control of a mobile robot: a user study," in *iros*, vol. 3, 2002, pp. 2867–2874 vol.3.

[10] H. Boschloo, T. Lam, M. Mulder, and M. van Paasen, "A collision avoidance system for a remotely-operated helicopter using haptic feedback," in *IEEE Int. Conf. on Systems, Man and Cybernetics*, The Hague, 2004, pp. 229–235.

[11] A. Fattouh, M. Sahnoun, and G. Bourhis, "Force feedback joystick control of a powered wheelchair: preliminary study," in *IEEE Int.Conf. on Systems, Man and Cybernetics*, vol. 3, Oct. 2004, pp. 2640–2645.

[12] S. Lee, G. S. Sukhatme, G. Jounghyun, and K. C. mo Park, "Haptic teleoperation of a mobile robot: A user study, presence: Teleoperators & virtual environments," 2005.

[13] G. Bourhis and M. Sahnoun, "Assisted control mode for a smart wheelchair," in *IEEE 10th Int. Conf. on Rehabilitation Robotics, ICORR*, June 2007, pp. 158–163.

[14] D. Lee and P. Li, "Passive coordination control of nonlinear bilateral teleoperated manipulators," *Robotics and Automation, 2002. Proceedings. ICRA '02. IEEE International Conference on*, vol. 3, pp. 3278–3283, 2002.

[15] D. A. Bell, S. P. Levine, Y. Koren, L. A. Jaros, and J. Borenstein, "Design criteria for obstacle avoidance in a shared control system," in *Proc. RESNA '94 Conference. Nashville*, 1994, pp. 17–24.

[16] E. Demeester, A. Huntemann, D. Vanhooydonck, G. Vanacker, H. Van Brussel, and M. Nuttin, "User-adapted plan recognition and user-adapted shared control: A bayesian approach to semi-autonomous wheelchair driving," *Auton. Robot.*, vol. 24, pp. 193–211, 2008.

[17] A. Hüntemann, "Probabilistic human-robot navigation," Ph.D. dissertation, K.U.Leuven, 2011, iSBN 978-94-6018-325-6.

[18] N. Tischler and A. Goldenberg, "Stiffness control for geared manipulators," in *Robotics and Automation, 2001. Proceedings 2001 ICRA. IEEE International Conference on*, vol. 3, 2001, pp. 3042 – 3046 vol.3.

[19] C. Carignan, M. Naylor, and S. Roderick, "Controlling shoulder impedance in a rehabilitation arm exoskeleton," in *Robotics and Automation, 2008. ICRA 2008. IEEE International Conference on*, may 2008, pp. 2453 –2458.

[20] H. Tan, J. Radcliffe, B. N. Ga, H. Z. Tan, B. Eberman, M. A. Srinivasan, and B. Cheng, "Human factors for the design of force-reflecting haptic interfaces," 1994.